The Influence of Carrier Air Preheating on Autoignition of Inline-Injected Hydrogen-Nitrogen Mixtures in Vitiated Air of High Temperature

Christoph A. Schmalhofer
German Aerospace Center (DLR)
Institute of Combustion Technology
Pfaffenwaldring 38-40
70569 Stuttgart, Germany
Email: Christoph.Schmalhofer@dlr.de

Peter Griebel
German Aerospace Center (DLR)
Institute of Combustion Technology
Pfaffenwaldring 38-40
70569 Stuttgart, Germany
Email: Peter.Griebel@dlr.de

Manfred Aigner
German Aerospace Center (DLR)
Institute of Combustion Technology
Pfaffenwaldring 38-40
70569 Stuttgart, Germany
Email: Manfred.Aigner@dlr.de

ABSTRACT

The use of highly reactive hydrogen-rich fuels in lean premixed combustion systems strongly affects the operability of stationary gas turbines resulting in higher autoignition and flashback risks. The present study investigates the autoignition behaviour and ignition kernel evolution of hydrogen-nitrogen fuel mixtures in an inline co-flow injector configuration at relevant reheat combustor operating conditions. High-speed luminosity and PIV measurements in an optically accessible reheat combustor are employed. Autoignition and flame stabilisation limits strongly depend on temperatures of vitiated air and carrier preheating. Higher hydrogen content significantly promotes the formation and development of different types of autoignition kernels: More autoignition kernels evolve with higher hydrogen content showing the promoting effect of equivalence ratio on local ignition events. Autoignition kernels develop downstream a certain distance from the injector, indicating the influence of ignition delay on kernel development. The development of autoignition kernels is linked to the shear layer development derived from global experimental conditions.

Nomenclature

AI Autoignition
BL Baseline Conditions
C Carrier
CFR Carrier-to-fuel mass flow ratio
F Fuel
GT Gas turbine
HG Hot gas generator
min Minimum value
MS Mixing section
SEV Sequential Environmental
stab Flame stabilisation
δ Shear layer thickness [mm]
Φ Equivalence ratio [-]
C_δ Constant for shear layer gradient [-]
p Pressure [bar]

T Temperature [K]
u Velocity [m/s]
X Normalised volume fraction [-]
x Horizontal coordinate [mm]
y Vertical coordinate [mm]

1 INTRODUCTION

Hydrogen-rich fuels can play a major role in achieving de-carbonisation targets in power generation systems with minimal CO_2-emissions and minimal environmental impact as requested in the COP 21 goals. Hydrogen-rich fuels derived from coal or biomass gasification together with a pre-combustion carbon capture process might be a solution to meet those requirements. Burning hydrogen-rich fuels in lean premixed combustion systems has a twofold impact on gas turbine (GT) operability. On the one hand, the operational range is widened due to the lower lean blow out limit of hydrogen-rich fuels. On the other hand, autoignition and flashback risks increase, compared to gas turbines operated on natural gas. In this context, ensuring operational reliability remains one of the key aspects of GT combustor design. Due to their higher reactivity, hydrogen-rich fuels pose significant challenges to the gas turbine design in terms of avoiding autoignition and flashback leading to flame stabilisation in combustor components, e.g. the premixing section, not designed to sustain higher thermal loads. For this reason the investigation of the beforehand mentioned phenomena is of high interest. This motivated the investigation of autoignition of hydrogen-rich fuels in a generic reheat combustor integrated in DLR Stuttgart's optically accessible high-pressure combustor rig, which offers the possibility to investigate those phenomena at gas turbine relevant operating conditions. In this rig, experiments with a wide range of optical and laser measurement techniques can be performed.
Local conditions favourable for autoignition have been shown to be strongly dependent on turbulent processes [1–4]. The effect of the turbulent fluctuations are twofold [1, 4], since local mixing can be improved and additional chemical pathways can be facilitated, while the time interval during which favourable conditions for autoignition exist ("excursion time" [1]) can be reduced. Additionally, the formation of autoignition kernels is influenced by other processes interacting with the local turbulence. Firstly, the pre-ignition reactions between fuel and oxidiser and secondly, the thermal runaway induced by the heat release and formation of radicals from those reactions [3]. Those autoignition kernels are found to develop at a certain mixture fraction, called the "most reactive mixture fraction" [2], which lies on the fuel lean side for hydrogen autoignition and obtains values between 0.01 and 0.1 [2]. Conditions favouring autoignition at the "most reactive mixture fraction" are present for low scalar dissipation rates and a low mixture fraction gradient, as it is particularly the case in vortex cores [2, 5], where fluid patches of high temperature and fluid patches of sufficient oxidiser or fuel content, respectively, are brought together by the strong mixing field. In addition, in those vortex cores the residence time of a sufficiently pre-mixed fluid parcel can be high enough and above the ignition delay time, which is another pre-requisite for the development of autoignition kernels. The third requirement for the development of autoignition kernels, a sufficiently high local mixture temperature above the autoignition temperature of the local mixture, is also a result of the local mixing process and strongly influenced by the turbulence-chemistry-interaction.

These investigations have primarily been conducted in lab-scale experiments that did not match conditions relevant for gas turbine operation, e.g. pressures of only up to 8 bar [4] or temperatures close to 1000 K [6]. Furthermore, those experiments were either conducted in homogeneous reactors or in co-flow systems with turbulence created by perforated plates, both not representative of a real GT application.
Various investigations of autoignition of hydrogen-nitrogen fuel mixtures at conditions relevant to gas turbine operation, e.g. in reheat combustion systems [7–9], have been conducted at DLR Stuttgart and have improved the understanding of the influences of pressure and temperature on autoignition events. The focus of these previous studies of a jet-in-crossflow configuration [10, 11] were fuel flexibility and investigations of autoignition kernels formation and their influence on flame stabilisation. In this configuration the turbulent flow field was dominated by the flow pattern related to the perpendicularly injected fuel jet and the accompanying horseshoe vortices which promote flame anchoring in the jet wake.
In a more recent investigation, in-line injector configurations using nitrogen as carrier medium, either premixed with the fuel or as a co-flow, were investigated [12]. The results showed that the autoignition limits are shifted to higher hydrogen volume fractions ($X_{H_2,min}$) due to the shielding effect of the inert carrier. Switching to air instead of nitrogen as a carrier medium significantly decreased the autoignition limits [13] due to the additional oxygen in the co-flow which promotes autoignition.

The present study mimics conditions relevant to gas turbine operation as they may occur e.g. in reheat systems [7–9]. Autoignition in the present study is investigated by high-speed luminescence imaging at recording rates of 30 kHz. This is fast enough to capture and resolve the formation process of autoignition kernels and to track their spatial and temporal development in the mixing section which happen on very short time scales and therefore require a high temporal resolution and excellent optical access. From these measurements together with theoretical analyses, such as the development of the shear

layers according to [14–16], an attempt is made to elucidate small-scale, localised processes that occur during autoignition in the mixing section. Together with the global mixing section parameters in terms of mixing section temperature, carrier air temperature and hydrogen volume fraction, the limits for autoignition and flame stabilisation are presented and the database of previous investigations [12, 13] is significantly expanded.
In this study, autoignition of hydrogen-nitrogen fuel blends is investigated for different carrier air preheating temperatures for the co-flow in-line injector configuration that has been already described in detail in [13]. Thanks to the carrier air preheating the present investigation is closer to industrial applications, e.g. GT reheat combustors, in which carrier air temperatures above ambient temperature are common. Autoignition limits in terms of minimal hydrogen volume fraction at which autoignition kernels occur for a given set of mixing section and carrier air temperatures are presented. A detailed analysis of the distribution of ”first” and ”stabilising” kernels in the mixing section is given and the influences of carrier air preheating temperature, mixing section temperature and hydrogen volume fraction on the formation of those kernels are discussed. In addition, the connection between global mixing section conditions, kernel origins and shear layer development is shown.

2 EXPERIMENTAL SETUP

The investigations were conducted in the high-pressure combustor rig (HBK-S) at the DLR Institute of Combustion Technology in Stuttgart. The rig is designed for investigating scaled combustors at high temperatures and pressures typical of GT operating conditions and offers extremely good optical access to the test section for the application of optical and laser diagnostics [17].

2.1 Reheat Combustor, Mixing Section and Fuel Injector

In Fig. 1 and 2 the optically accessible reheat combustor and a sketch of the co-flwo injector are shown. The test carrier consists of the three main parts, hot gas generator (HG), mixing section (MS) and reheat combustion chamber. The high-temperature vitiated air conditions are generated in the hot gas generator by a natural gas fired FLOX® [18] burner and admixed dilution air at ambient temperature. This yields hot gas conditions typical for technical combustion systems, e.g. in reheat combustors, in terms of temperature, pressure, velocity and oxygen content. The hot gas generator was operated at air preheating temperatures between 623 K and 773 K and equivalence ratios of 0.40 - 0.43, resulting in a thermal power of 420 kW [18]. More details can be found in [13].

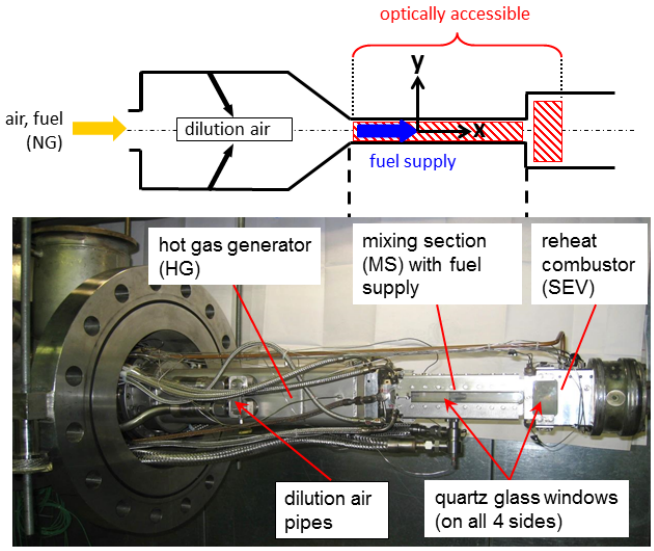

Fig. 1: OPTICALLY ACCESSIBLE REHEAT COMBUSTOR AT DLR STUTTGART.

The mixing section, a square duct of 25 x 25 mm^2 cross section, is equipped with quartz glass windows on all four sides to allow for very good optical access from 100 mm upstream to 110 mm downstream of the fuel injector. A sudden expansion of the cross section to $70\,x\,70\,mm^2$ at the reheat combustor entry induces an outer recirculation zone for flame stabilisation [13]. A hydrogen/ nitrogen mixture with a set point value of 70 vol. % hydrogen and 30 vol. % nitrogen resulting in a global equivalence ratio of $\Phi = 0.40$ was injected into the mixing section. The fuel mixture of ambient temperature was injected in-line with the hot gas flow on the axis of symmetry of the mixing section as indicated by the blue arrow in Fig. 1. A

co-flow fuel injector [13] shown in Fig. 2 was investigated in the present study. The H_2/N_2-fuel mixture was embedded in a preheated carrier-air co-flow, representing carrier-air conditions of technical applications. The inner flow channels of the injector were designed not to exceed subsonic conditions in the throat at the position of the flow straightener. The fuel injector can be seen as a representative single port of a fuel injector array in a real engine.

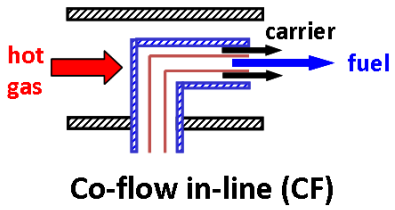

Fig. 2: SCHEMATIC OF THE CO-FLOW IN-LINE INJECTOR CONFIGURATION IN THE MIXING SECTION.

2.2 Operating Conditions and Mixing Section Inlet Conditions

The baseline (BL) operating conditions in the mixing section were defined corresponding to GT relevant reheat operating conditions for hydrogen-rich fuels. The bulk flow velocity was 200 m/s at a pressure of 15 bar and a relative temperature of T_{MS}/T_{BL} = 1. The oxygen content of the hot gas was held constant at about 15 vol. % O_2, measured by an exhaust probe located at the mixing section inlet and controlled by the HG equivalence ratio and the amount of ad-mixed dilution air in the hot gas generator. The mixing section temperature (T_{MS}) was set to its target values by adjusting the dilution air mass flow rate. In the autoignition measurements the mixing section temperature, in relation to the mixing section temperature at baseline conditions (T_{BL}), was varied between $0.93 \leq T_{MS}/T_{BL} \leq 1.07$. The fuel blend with a set point value of 70/30 vol. % H_2/N_2 ($\Phi = 0.40$) has been selected in accordance with the European Union framework 6 project ENCAP [19, 20] guidelines for achieving carbon-capture targets of up to 90 % carbon capture in an IGCC-CCS plant. The mass flow rate of carrier air was calculated with a fixed set point carrier-to-fuel mass flow ratio (CFR) of 1.0 for all measurement points. The carrier air was preheated to temperatures of 303 K, 523 K, 573 K, 623 K and 703 K in order to mimic real gas turbine conditions [7–9]. During the experiments the bulk velocity and the oxygen content were kept constant at 200 m/s and 15 $\pm$ 0.5 vol. %, respectively.

2.3 Measurement Techniques

Autoignition events were studied by recording the luminosity of autoignition kernels in the mixing section downstream of the fuel injector exit plane using high-speed cameras (LaVision® HSS 6 and HSS 8) as already employed in previous studies [12, 13]. Minor changes to the camera set-up were made in order to expand the recording time to 1.5 sec at 30 kHz, resulting in 30.000 images recorded prior to and 15.000 images after the trigger signal by setting the cameras to pre-triggering mode.

The mixing section temperature was recorded at the mixing section inlet by means of a shielded singe thermocouple as described in detail in [17].

The velocity field in the mixing section was measured by Particle Image Velocimetry (PIV) with Titanium-dioxide (TiO_2) particles as flow tracers. The particles had a nominal diameter of about 1.0 µm and were illuminated by a double-pulse dual cavity Nd:YAG laser (wavelength: 532 nm, pulse energy: 2 x 120 mJ, pulse separation: 2 µs - 3 µs). The laser light sheet of about 1.0 mm thickness was introduced into the mixing section symmetry plane from the top and the particle images were recorded from the right hand side (streamwise direction) by a CCD camera. The double-frame CCD camera recorded the images at a rate of 5 Hz and a resolution of 1600 x 1200 pixels. Ambient light suppression was ensured by a band pass filter (532 $\pm$ 10 nm) on the camera lens (focal length: 50 mm, f# = 5.6). The TiO_2 tracer particles were added to the dilution air, the carrier air and the nitrogen in the fuel mixture in order to ensure homogeneous seeding and a high resolution of the velocity field in the whole mixing section. Spatial resolution of 1.1 mm was achieved which corresponds to an interrogation window size of 16 x 16 pixels. A commercial cross-correlation algorithm from LaVision Davis 8® was used to calculate the velocity vector fields. For further information on the PIV setup see [17, 21]. The PIV measurements were obtained at conditions at which autoignition events could be expected in the mixing section according to already established autoignition limits. Since autoignition leads to SEV fuel shut down and therefore to a change in the local velocity distribution, no hydrogen was injected in the mixing section during the PIV measurements in order to avoid autoignition. To keep flow properties such as jet momentum ratio between fuel and carrier at the desired values of the autoignition event, the hydrogen mass flow was replaced by the equivalent nitrogen mass flow.

3 RESULTS AND DISCUSSION

For the discussion of autoignition the classification of "first", "subsequent" and "stabilising" kernels already established in previous work [13] is used.

The "first" kernels occur at the minimum hydrogen volume fraction $X_{H_2,min} = f(T_{MS}, T_C)$ and mainly depend on the mixing section inlet conditions. These kernels are used to determine the autoignition limit for a certain mixing section temperature and carrier air temperature.

The "subsequent" kernels form either at the same minimum hydrogen volume fraction, but after the "first" kernel or at higher hydrogen contents at constant global mixing section parameters (pressure, mixing section temperature, carrier preheating temperature). Therefore, they might be also influenced by a change in local conditions (T, u, Φ) due to preceding kernels or due to the higher hydrogen mass flow injected into the mixing section or both. "First" and "subsequent" kernels are both convectively transported downstream out of the mixing section.

Finally, the "stabilising" kernels are a sub-type of the "subsequent" kernels since for constant T_{MS} and T_C they occur at hydrogen volume fractions much higher than the autoignition limit ($X_{H_2,stab} > X_{H_2,min}$) and initiate a non-interrupted sequence of autoignition kernels which finally lead to a stable flame in the mixing section. Since the typical development process of "first" and "stabilising" kernels has already been illustrated by high-speed luminosity images in [12, 13], this is set aside in the present paper. Flame stabilisation in the mixing section of a real GT must be prevented since the mixing section is not designed to sustain higher thermal loads thereby risking irreversible damages, GT failures and the need for cost-intensive repairs. This motivated the present work on autoignition in order to understand the formation and development processes of the different kernel types in detail and from this to derive design guidelines for a safe and reliable GT operation. Since "first" kernels correspond to the autoignition limits for certain mixing section conditions (p_{MS}, T_{MS}, T_C), understanding the formation and development of the "first" kernel is necessary to derive GT operation limits at which no autoignition will occur, thereby inherently securing safe GT operation. In addition, the "stabilising" kernel is the "critical" condition at which a save GT operation is impossible, a fact that necessitates the precise understanding of the mechanisms leading to flame stabilisation in the mixing section.

While previous studies have been either dealing with the effect of different fuel injector configurations (jet-in-crossflow, premixed, co-flow) on autoignition using nitrogen as a carrier medium [12] or elucidating the influence of switching from nitrogen to carrier air of ambient temperature [13], the present investigation focuses on autoignition using preheated carrier air in the co-flow injector. The carrier air was preheated to temperatures of 523 K, 573 K, 623 K and 703 K in order to investigate the influence of carrier preheating on autoignition.

Firstly, the autoignition limits are presented and discussed. Secondly, the global distributions of the "first" and "stabilising" kernels at all measured conditions are presented, followed by the discussion of the influences of the temperature and hydrogen volume fraction on the distribution of the two kernel types.

3.1 Influence of Carrier Air Temperature on Autoignition Limits

The autoignition limits show a reciprocal dependence on mixing section temperature at all carrier air preheating temperatures investigated, see Fig. 3. For a higher mixing section temperature autoignition occurs at a lower minimum hydrogen volume fraction $X_{H_2,min}$. While previous investigations [12, 13] have already shown the same trend, the present study significantly extends the database to more extreme mixing section temperatures and does include elevated carrier air temperatures. Based on this wider data basis a reciprocal exponential dependence of the autoignition limits on temperature is claimed. The negative curvatures of the lines of best fit, shown for T_C=303 K and 703 K in Fig. 3, illustrate that the dependence on the mixing section temperature decreases with increasing mixing section temperature. This means that the autoignition limit at higher mixing section temperatures is not very sensitive to hydrogen volume fraction. The equations for the lines of best fit are $7.691 \times 10^3 \cdot \exp\left(-10.26 \cdot \frac{T_{MS}}{T_{BL}}\right)$ for T_C=303 K and $2.634 \times 10^4 \cdot \exp\left(-11.70 \cdot \frac{T_{MS}}{T_{BL}}\right)$ for 703 K, respectively. Increasing the carrier air preheating temperatures does not seem to have a significant influence on autoignition limits. Only at very high preheating temperatures above 623 K (green and red markers in Fig. 3) and relative mixing section temperatures $\frac{T_{MS}}{T_{BL}}$ below 0.98, autoignition limits occur at slightly lower $X_{H_2,min}$ values than for the other cases. At first glance, this may seem counter-intuitive, since from autoignition theory higher temperatures are expected to promote the development of autoignition spots. From the experimental conditions, the mass flow ratio between hot gas flow at T_{MS} and carrier air mass flow at elevated T_C is typically about 20:1. This means the mixing section temperature has a dominant influence on local temperature in the mixing section. Only for very high carrier air preheating temperatures and lower T_{MS} values associated with higher hydrogen volume fractions at autoignition limits (and therefore higher hydrogen mass flow rates) a slight influence of carrier air temperature on AI limits can be observed.

The stabilisation limits seem to be independent from the mixing section temperature and the carrier air preheating temperature, Fig. 3. Flame stabilisation only occurs at hydrogen volume fractions above 42 vol. %, even for the highest carrier air preheating temperature investigated. As stated above, the "stabilising" kernels initiate flame stabilisation and occur with preceding kernels present in the mixing section. Therefore, an influence of those predecessors is very likely, which could explain the different behaviour compared to "first" kernels.

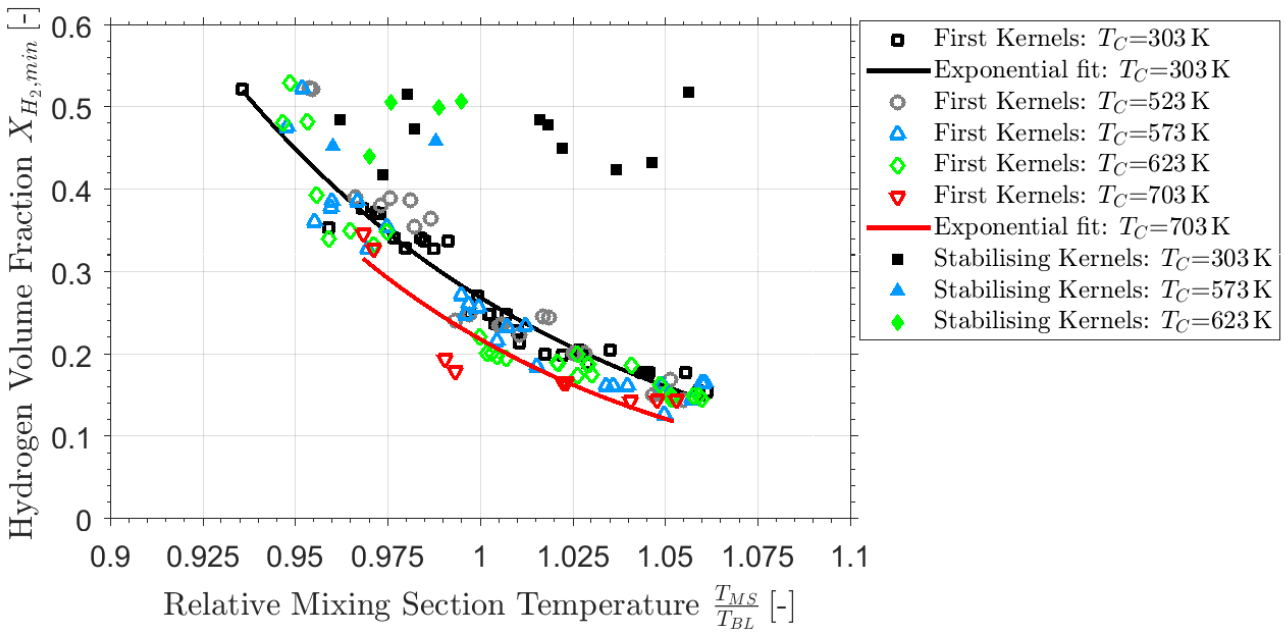

Fig. 3: AUTOIGNITION LIMITS (×) AND FLAME STABILISATION LIMITS (▲) FOR DIFFERENT CARRIER PREHEATING TEMPERATURES.

The results from Fig. 3 yield valuable design guidelines for GT operation. For safe and reliable GT operation flame stabilisation in components not designed to sustain high thermal loads, like the mixing section, must be avoided under any circumstances, because even for a very short time interval flame stabilisation will lead to irreversible mechanical damage and failure of the gas turbine. In order to avoid flame stabilisation, hydrogen volume fractions up to 40 vol. % can be tolerated even at elevated carrier preheating temperatures up to 623 K, when the mixing section conditions are slightly de-rated, e.g. to a lower relative mixing section temperature of approximately 0.94. Although autoignition occurs at significantly lower hydrogen volume fractions as low as 12 vol. % for higher $\frac{T_{MS}}{T_{BL}}$ values, e.g. 1.06, the corresponding autoignition kernels are convected out of the mixing section and there is still a significant margin until the flame stabilisation limit is reached.

3.2 Global Distribution of Autoignition Kernels

Figure 4 shows the distribution of the "first" kernels in the mixing section in x- and y-direction for different carrier air temperatures. Please note that each kernel corresponds to one combination of mixing section temperature and carrier air temperature. No discernible influence of carrier air preheating on the location of the "first" kernels can be seen. They are almost evenly distributed in x-direction whereas in y-direction most of the kernels are concentrated in the lower part of the mixing section between the centre line (y = 0 mm) and y = -10 mm. It is woth mentioning that an axis-symmetric kernel distribution can only be expected for a large number of autoignition experiments in order to obtain statistical results representing the stochastic nature of autoignition. Due to the large time period needed for a single autoignition run, this was not feasible in the present investigations. Therefore, the limited number of autoignition runs does not cover statistical results. In addition, the inhomogeneity might originate from a slightly inhomogeneous fuel jet velocity distribution at the injector exit plane caused by flow separation inside the injector due to the bent tube, although perforated plates were used in the fuel and carrier air flow channel to minimize these effects.
For all conditions investigated a lower axial boundary seems to establish approximately 20 mm downstream the injector exit plane. Kernels occur only downstream of this lower boundary because sufficiently premixed fluid parcels of fuel and hot oxidiser at the proper local temperature and local stoichiometry must be formed for autoignition, requiring a certain amount of time in which those parcels travel the equivalent distance in the mixing section. Furthermore, the residence time of the fluid parcel under those conditions must be equal or longer than the required ignition delay time. A rough estimation using the bulk velocity value of 200 m/s and the axial distance of 20 mm results in a residence time of about 0.1 ms which is shorter than the kinetic ignition delay time of a homogeneous mixture of about 0.3-0.7 ms [11]. This is in accordance to the results in [1], stating that in a real turbulent system the ignition delay time tends to be shorter than the one in a homogeneous reactor.

"Stabilising" kernels were recorded for three different carrier air temperatures: T_C = 303 K, 573 K and 623 K, Fig. 4. Due to the high thermal load in the mixing section in case of flame stabilisation only a few events were recorded in order to prevent thermal damage of the test rig. The "stabilising" kernels, Fig. 4, are distributed over a wide range in both x- and y-direction.

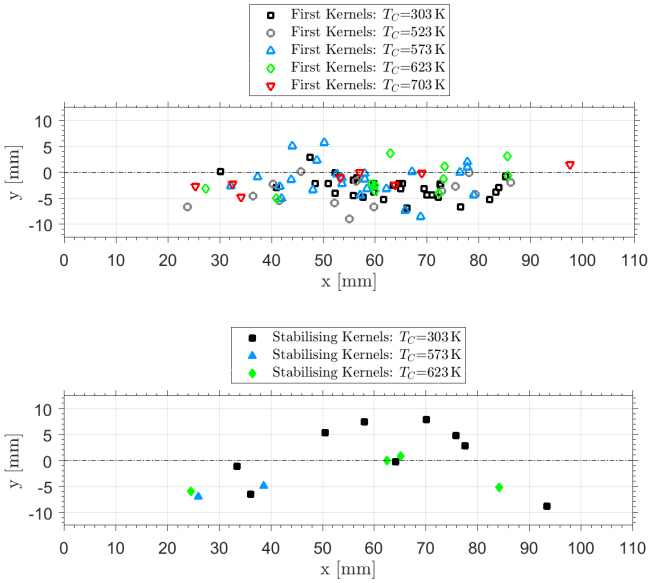

Fig. 4: GLOBAL DISTRIBUTION (SIDE VIEW) OF THE "FIRST" (×) AND "STABILISING" KERNELS (▲) IN THE MIXING SECTION FOR DIFFERENT CARRIER AIR PREHEATING TEMPERATURES T_C.

No clear dependence on the carrier air preheating temperature is found, as in the case of the "first" kernels. Furthermore, "stabilising" kernels form downstream of the axial limit of x = 20 mm. This result is manifested for "subsequent" kernels as well, the corresponding distributions are shown in Fig. 5. Please note that the different amount of "subsequent" kernels for different preheating temperatures results from a different number of experiments for each condition.

Downstream from x = 20 mm the "subsequent" kernels develop over the full range, both, in x- and y-direction, which is true for all mixing section temperatures and carrier preheating temperatures investigated. Upstream of x = 20 mm no "subsequent" kernel is found for the reason already explained above. In addition, as the distributions of the "subsequent" and "stabilising" kernels clearly show, a higher hydrogen volume fraction above the autoignition limit as well as the potential influence of preceding kernels in the mixing section do not affect this boundary which consolidates the explanation given above.

3.3 Influence of Mixing Section Temperature and Hydrogen Volume Fraction on the Distribution of "First" and "Stabilising" Kernels

In order to better understand the autoignition kernel formation, the influence of mixing section temperature T_{MS} and hydrogen volume fraction X_{H_2} on the kernel distribution for different carrier air preheating temperatures was investigated in detail regarding the "first" and the "stabilising" kernels. For the sake of clarity, only the results for carrier preheating temperatures of 303 K, 573 K and 623 K are shown, since for these cases "stabilising" kernels were obtained as well. The conclusions regarding the "first" kernels also hold true for the other two preheating temperatures not presented here.

Kernel distribution in x-direction

In Fig. 6 the x-coordinate of the "first" and "stabilising" kernels as a function of the mixing section temperature T_{MS} and the hydrogen volume fraction X_{H_2} is shown. At a higher mixing section temperature T_{MS} and constant carrier air temperature T_C "first" kernels occur further upstream in the mixing section, but remain downstream of the previously described limit at x = 20 mm. For a higher T_C and constant T_{MS} the "first" kernels tend to occur further upstream as well. The influence of the mixing section temperature is clearly dominating the one of the carrier preheating temperature.
Increasing hydrogen volume fractions at which "first" kernels occur seem to shift the kernel x-positions downstream. This effect is stronger for lower carrier air preheating temperatures, which means at lower T_C a certain increase in hydrogen volume fraction yields a larger downstream shift of the "first" kernels than for higher preheating temperatures.
Both results illustrate the promoting effect of temperature on autoignition. Autoignition does strongly depend on the local conditions a fluid parcel is exposed to in addition to its trajectory. In order for autoignition to occur, the temperature must exceed the autoignition temperature of the mixture with sufficient mixing in terms of a sufficiently high local mixture fraction and with residence times longer than the ignition delay time. The mixing section and carrier preheating temperatures and

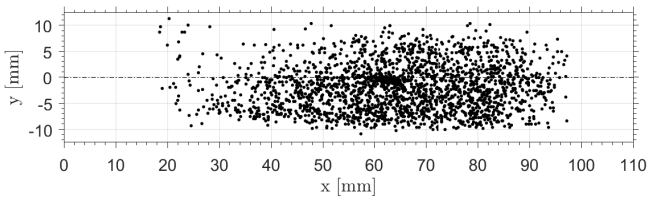

(a) T_C=303 K

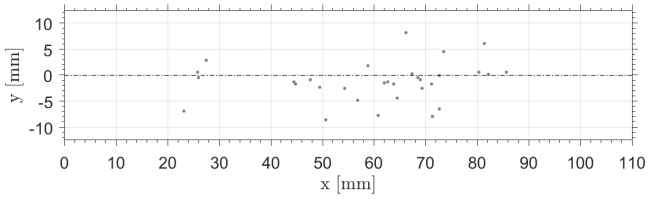

(b) T_C=523 K

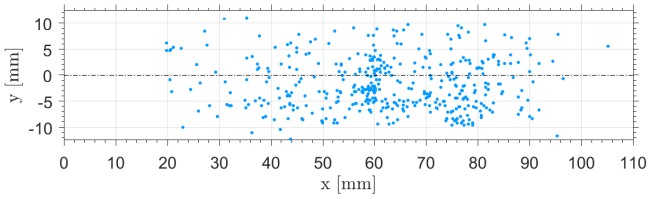

(c) T_C=573 K

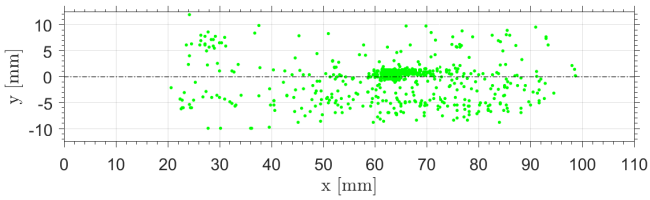

(d) T_C=623 K

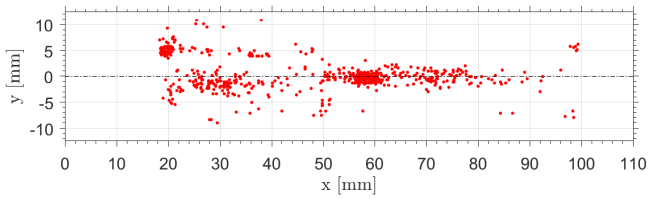

(e) T_C=703 K

Fig. 5: GLOBAL DISTRIBUTION (SIDE VIEW) OF THE "SUBSEQUENT" KERNELS IN THE MIXING SECTION FOR DIFFERENT CARRIER AIR PREHEATING TEMPERATURES T_C

the hydrogen volume fraction are global parameters and the local temperature at an arbitrary location in the mixing section will likely differ from them due to the turbulent mixing process. Nevertheless, global parameters will dominantly influence the local conditions. Higher mixing section and carrier temperatures result in higher local temperatures, which is further amplified by lower amounts of hydrogen at ambient temperatures injected into the mixing section at higher T_{MS}, as shown in for the "first" autoignition kernels in Fig. 3. This facilitates autoignition of sufficiently premixed fluid parcels because of a lower ignition delay time due to a higher temperature, consequently shifting the location at which "first" kernels occur further upstream.

Higher hydrogen volume fractions correspond to lower mixing section temperatures for the occurrence of "first" kernels in the mixing section, Fig. 3, consequently the downstream shift of the kernel positions with increasing hydrogen volume fraction, Fig. 6, supports the above findings. Regarding the hydrogen volume fraction alone, these results seems to be counter-intuitive at first glance, since higher hydrogen contents mean higher global equivalence ratios. These conditions are likely to lead to a higher reactivity of the local fuel/ oxidiser/ hot gas mixture because in addition the fuel jet velocity is higher for a higher H_2 content resulting in a larger relative velocity gradient between fuel and carrier air promoting turbulent mixing due to stronger

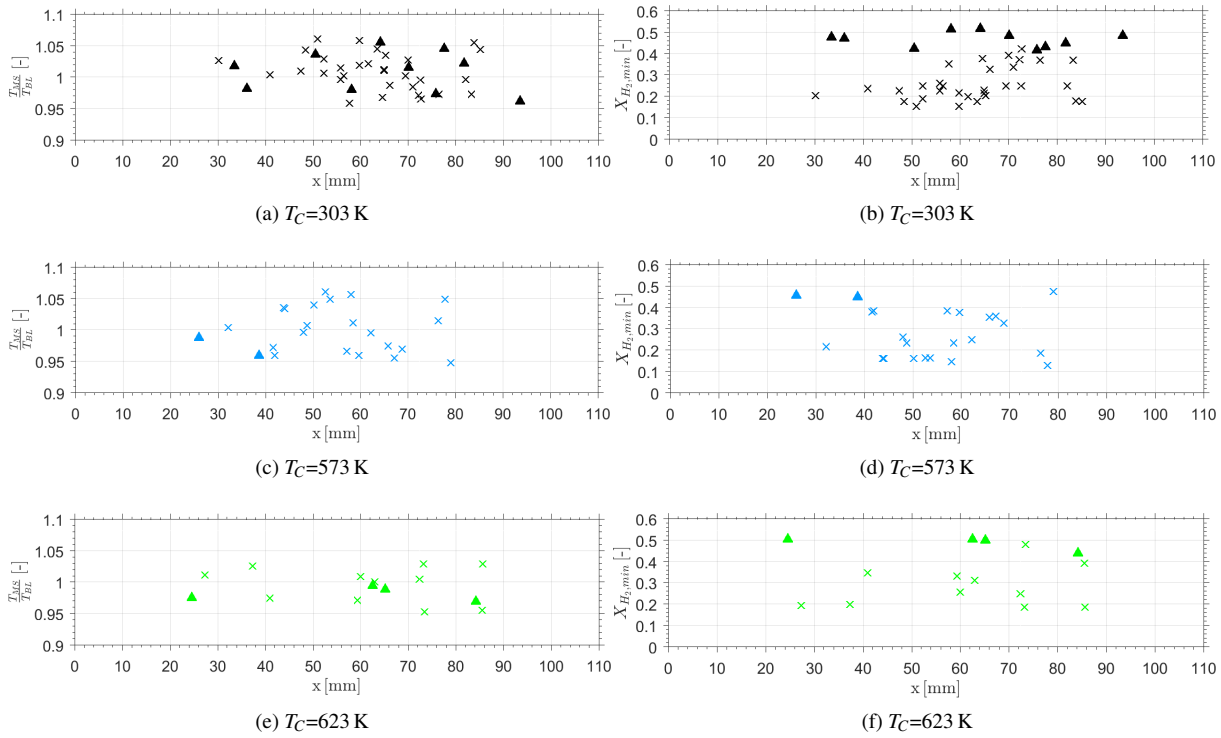

(a) T_C=303 K (b) T_C=303 K

(c) T_C=573 K (d) T_C=573 K

(e) T_C=623 K (f) T_C=623 K

Fig. 6: DISTRIBUTION IN X-DIRECTION (SIDE VIEW) OF THE "FIRST" (×) AND "STABILISING" (▲) KERNELS FOR DIFFERENT CARRIER AIR PREHEATING TEMPERATURES AS FUNCTION OF MIXING SECTION TEMPERATURE T_{MS} (a, c, e) AND AS FUNCTION OF HYDROGEN VOLUME FRACTION X_{H_2} (b, d, f).

shear. Thereby, higher reactivity is supposed to promote autoignition. The increase in hydrogen volume fraction cannot be investigated separately from the corresponding decrease in mixing section temperature, and therefore from their influence on the local mixing temperature. As Fig. 6 implies, the x-position of the "first" kernels shows a strong temperature dependence which seems to clearly dominate the influence of local mixture fraction and equivalence ratio. Furthermore, additional injection of hydrogen mass flow is connected to several effects [1, 4] partly favourable, partly non-favourable to autoignition. On the one hand, higher reactivity leads to a larger radical pool and higher turbulent fluctuations can improve local mixing and facilitate new kinetic pathways. On the other hand, a higher jet momentum can also lead to a decrease in "excursion" time [1] and higher scalar dissipation rates and diffusive transport which will move radicals away from favourable autoignition spots. The present investigations cannot dissolve these local phenomena, but they have to be kept in mind when interpreting autoignition results of "first" kernels.

In contrast to "first" kernels, "stabilising" kernels are distributed along the whole mixing section length downstream of x = 20 mm. No further predisposition in x-direction can be seen, although for the same mixing section conditions (T_C, T_{MS} or $X_{H_2,min}$) they seem to develop further upstream than the "first" kernels. As stated above, "stabilising" kernels do not exclusively depend on the initial local conditions in the mixing section, because preceding kernels already occurred in the mixing section the heat release of which is likely to have changed the conditions under which "stabilising" kernels develop. As a consequence, "stabilising" kernels are subject to additional aero-thermodynamic influences that cannot be dissolved in the present experiments.

Kernel distribution in y-direction

At low mixing section temperatures and low carrier air preheating, "first" kernels are distributed in the lower half of the mixing section, Fig. 7. For higher mixing section or carrier air preheating temperatures the kernels occur closer to the mixing section centre line. It is visible that the effect of the mixing section temperature is stronger than the one of the carrier air preheating. An increase in hydrogen volume fraction leads to a larger distance of the "first" kernel in y-direction from the centre line. Meanwhile, increasing carrier preheating shifts the y-position of the kernels towards the centre line. Again, the effect of the mixing section temperature dominates the one of the carrier preheating temperature clearly. One would expect a statistically equal distribution around the centre line for a sufficiently large number of autoignition events in an ideally sym-

metrical duct flow. Deviation from the perfectly symmetric distribution of kernels can be dedicated to the limited number of autoignition measurements (due to restrictions in measurement time) and a small inhomogeneity of the fuel jet velocity at the exit plan already mentioned earlier.

The "stabilising" kernels can be found across the entire height of the mixing section. Their origin does not seem to directly depend on the initial mixing section conditions (T_{MS}, T_C, X_{H_2}). This once more clearly illustrates the underlying difference in development mechanisms between "first" and "stabilising" kernels. The former are dominantly influenced by the initial global mixing section parameters and the resulting local conditions downstream of the injector, while the latter seem to be significantly influenced by a change in local and global mixing section conditions which the preceding kernels and their associated heat release and change of aero-thermodynamics of the duct flow field result in.

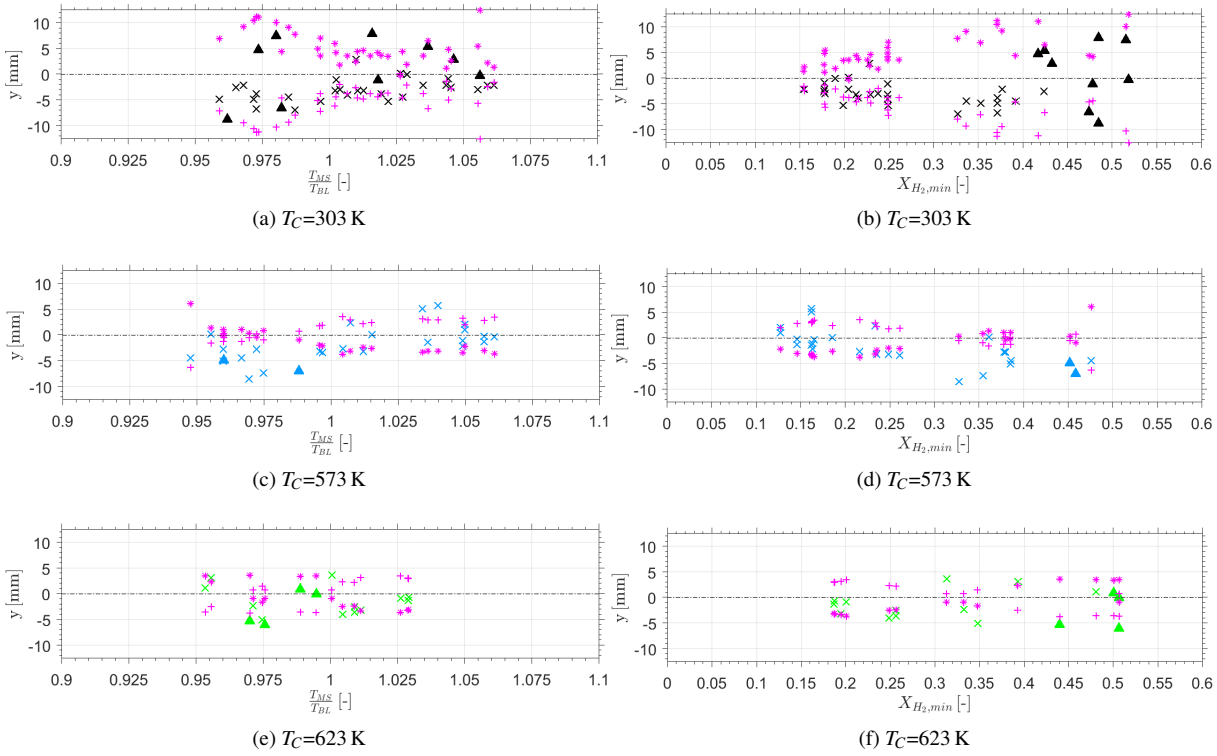

(a) T_C=303 K (b) T_C=303 K

(c) T_C=573 K (d) T_C=573 K

(e) T_C=623 K (f) T_C=623 K

Fig. 7: DISTRIBUTION IN Y-DIRECTION (SIDE VIEW) OF THE "FIRST" (×) AND "STABILISING" (▲) KERNELS AND UPPER (+) AND LOWER (*) SHEAR LAYER BOUNDARIES FOR DIFFERENT CARRIER AIR PREHEATING TEMPERATURES AS FUNCTION OF MIXING SECTION TEMPERATURE T_{MS} (a, c, e) AND AS FUNCTION OF HYDROGEN VOLUME FRACTION X_{H_2} (b, d, f).

Shear layer development and lateral kernel position

To get a better insight into the influence of initial global mixing section conditions on the development of the "first" kernels, Fig. 7 also shows the shear layer boundaries in the mixing section for each kernel at the respective mixing section temperature and hydrogen volume fraction. The theory of mixing in a turbulent reactive shear layer flow was derived mainly by [14–16] and [22–24]. In [14] the following equation for the calculation of the shear layer gradient is given.

$$\frac{\delta(x)}{x} = C_\delta \cdot \left(\frac{1-r}{1+\sqrt{s}\cdot r}\right) \cdot \left(1+\sqrt{s}-\frac{1-\sqrt{s}}{1+2.9\cdot\frac{1+r}{1-r}}\right) \tag{1}$$

This equation together with $C_\delta = 0.37$ [16] was used to calculate the shear layer boundaries plotted in Fig. 7. The distribution of the axial velocity in the mixing section shown in Fig. 8 was obtained from PIV measurements for autoignition at baseline conditions. The inner shear layer boundary developing according to Eqn. 1 due to the velocity ratio $\left(r_{FC} = \frac{u_F}{u_C}\right)$ and

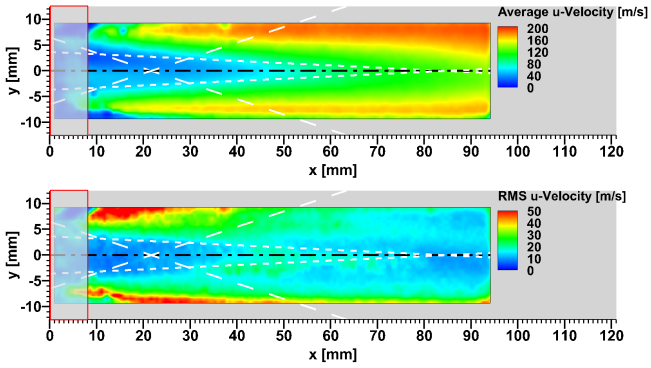

Fig. 8: VELOCITY DISTRIBUTION (TOP: AVERAGE VALUES, BOTTOM: RMS-VALUES) IN X-Y-PLANE FROM PIV MEASUREMENTS. WHITE LINES INDICATE THE DEVELOPMENT OF THE INNER BOUNDARIES OF THE INNER SHEAR LAYER BETWEEN FUEL AND CARRIER FLOW (SHORT DASHED LINES) AND THE OUTER SHEAR LAYER BETWEEN CARRIER AND HOT GAS FLOW (LONG DASHED LINES) ACCORDING TO [14].

density ratio $\left(s_{FC} = \frac{\rho_F}{\rho_C}\right)$ between the fuel and carrier air flow is marked with short dashed lines. The shear layer boundary between carrier air and hot gas flow (long dashed lines) was obtained analogously. Very good agreement between theory and experiment can be seen in Fig. 8 for the inner shear layer boundary between fuel and carrier air flow. The shear layer boundaries coincide well with those regions in which the maximum gradients of the "Root-Mean-Square (RMS)"-values of the velocity in x-direction are found. Furthermore, the cone shaped region of lower axial velocities representing the fuel jet core is well visible outside the shear layer boundaries in the averaged velocity distribution. The shear layer between the carrier air and hot gas flow develops with a much steeper gradient due to the large velocity ratio between the two flows and obviously merges into the inner shear layer between fuel and carrier air flow. Due to laser light reflection at the metal surface of the fuel injector in the near field region (x $<$ 8 mm) this cannot be reproduced well by the PIV results and is marked by semi-transparent boxes in Fig. 8.

Due to the good agreement between theory and PIV results the transfer of the theoretical considerations for the inner shear layer development between fuel and carrier air flow to the "first" kernel origins is possible.
As Eqn. 1 indicates, the shear layer gradient increases with a higher velocity ratio and decreases with a higher density ratio. The sensitivity to a change in velocity ratio is higher than to a change in density ratio. Therefore, an increase in hydrogen volume fraction due to an increase in hydrogen mass flow results in a higher velocity ratio r_{FC} and therefore in a larger shear layer gradient. A twofold influence of higher carrier air preheating temperatures can be stated. Firstly, the density ratio is increased thereby decreasing the shear layer gradient. Secondly, the increase in density ratio decreases the velocity ratio leading again to a smaller shear layer gradient. An increase in mixing section (hot gas) temperature primarily influences the outer shear layer gradient between the hot gas and carrier air flow. Please note that any change in mixing section temperature is always connected to a change in the hydrogen volume fraction at which a "first" autoignition kernel forms, Fig. 3. Therefore, the influence of T_{MS} is indirectly seen through a change in r_{FC}.
The y-coordinate of the shear layer boundary at the corresponding position of each "first" kernel is obtained by calculating the shear layer gradient from the velocity and density ratios using the respective T_C, T_{MS} and X_{H_2} values and multiplying the result with the respective x-coordinate of the "first" kernel at the relevant mixing section conditions. The upper boundary of the inner shear layer between the fuel and carrier air flow starts in the upper half of the mixing section and the lower boundary in the lower half, respectively. Both boundaries are marked separately in Fig. 7. As soon as the upper boundary reaches the lower half of the mixing section $y < 0$ mm, and vice versa , the shear layer boundaries have merged as it is the case for x $>$ 80 mm in Fig. 8.
Note that the shear layer thickness corresponding to each "first" kernel position depends firstly on the corresponding shear layer gradient as a function of the respective velocity and density gradients. Secondly, it depends on the x-position of the respective kernel. Thus, the development of the shear layer thickness for changing mixing section or carrier air preheating temperature and changing hydrogen volume fraction must be derived from the shift in x-position due to different T_C, T_{MS} and X_{H_2} values and from their effects on the shear layer gradient at the same time. For example, a higher hydrogen volume fraction results in a higher velocity ratio and therefore in an increase in the shear layer gradient, Eqn. 1. At the same time, it leads to "first" kernel positions that are located further downstream, Fig. 6. The result of the higher shear layer gradient and the larger x-coordinate yields a higher shear layer thickness at the respective position in the mixing section.

Figure 7 shows that most of the "first" kernels lie within the shear layers or close to the shear layer boundaries for all mixing

section and carrier preheating temperatures and hydrogen volume fractions with the trends pointed out above. They develop in regions which are strongly influenced by large scale vortices [14, 16] and the vortex-driven entrainment of irrotational free-stream fluid into those vortices. As a consequence, the rotating motion that dominates the growing shear layers is impressed on the fluid parcels ("diastrophy" [14]) and mixing processes between fuel-dominant parcels and oxidator-dominant ones across the parcels' interfaces are enhanced due to shear. Fluid of high temperature and of high fuel or oxidator content is mixed in these vortices which due to their low scalar dissipation rate at the vortex cores [2] promote conditions which can facilitate autoignition and the development of "first" kernels. In these vortex cores pre-ignition reactions [3] can take place more easily due to the low scalar dissipation rate and low mixing fraction gradient [16] which will increase the radical pool available for an autoignition event.
The close connection between the positions of the "first" kernels in y-direction and the shear layer boundaries clearly shows that the formation mechanism of the "first" kernels is closely linked to the flow field and especially to the development of the shear layers. The initial mixing section conditions have a significant influence on the flow field and on the shear layer boundaries in particular and therefore on the formation of the "first" ignition kernels in y-direction. Furthermore, the distribution of the "first" kernels in x-direction is primarily subject to the balance between fluid parcel residence time and kinetic ignition delay time. While the former is a result of the trajectory of a fluid parcel in the mixing section and of the vortical fluid motion within the shear layers, the latter results primarily from the local mixing section temperature which is a function of both, the mixing section and the carrier preheating temperature.

The stabilising kernels also develop inside the shear layers, but a significant difference exists in comparison to the "first" kernels and the corresponding shear layer thickness. The "stabilising" kernels at correspondingly high hydrogen volume fractions develop at locations where the shear layers from the upper and the lower half of the mixing section have already merged. This can be seen as the shear layer boundary starting in the lower half of the mixing section is found at higher y-values than the one starting in the upper half. Clearly, the large scale vortices from both shear layers will interact and merge which renders the flow field dominated by three-dimensional effects and high degrees of mixing and entrainment of fluid into the vortices. Furthermore, assuming that the heat release associated with the predecessors of the "stabilising" kernels influences the flow field and the shear layer development, additional aero-thermodynamic effects come into play [23]. The depicted shear layer boundaries for "stabilising" kernels must be looked at with extreme caution, still they illustrate well that "stabilising" kernels develop under significantly different local and global conditions than "first" kernels and are most likely influenced by heat release and the corresponding aero-thermodynamic effects from their predecessors, which will require additional future investigations beyond the scope of the present study.

4 SUMMARY AND CONCLUSIONS

The focus of the present paper is the influence of carrier air preheating on autoignition of hydrogen-rich fuel mixtures at high-temperature vitiated air conditions using a co-flow injector. In addition, the autoignition limit database of previous studies is significantly extended to represent a wider range of mixing section temperatures. For all carrier air temperatures investigated a reciprocal dependence of the minimum hydrogen volume fraction on mixing section temperature leading to "first" autoignition kernels, defined as autoignition limits, is found. Only for carrier air preheating temperatures higher than 623 K and relative mixing section temperatures below 0.98 slightly lower autoignition limits are measured. "Stabilising" kernels, initiating a stable flame in the mixing section, occur at much higher hydrogen volume fractions and no influence of mixing section or carrier air preheating temperature is observed. From the presented autoignition and flame stabilisation limits design guidelines for a safe and reliable GT operation can be derived in order to prevent thermal damage of the mixing section by flame stabilisation.
The positions of "first" and "stabilising" kernels were analysed using high-speed luminescence measurements and PIV measurements. The mixing section temperature exerts a dominant influence on the position of the "first" ignition kernels in stream-wise direction, as higher temperatures reduce ignition delay times and thereby facilitate the formation of "first" ignition kernels further upstream. Furthermore, "first" autoignition kernels form and develop within the downstream moving vortices in or close to the shear layer boundaries, where at the vortex cores due to low scalar dissipation rates and low gradients of the local mixture fraction favourable conditions for autoignition in terms of temperature, sufficient mixing and sufficiently long residence times exist. The shear layer development depends on the initial mixing section conditions and the resulting velocity and density ratios and their effect upon shear layer growth. As a consequence, the formation of the "first" ignition kernels depends strongly on initial mixing section conditions.
In contrast, a different mechanism of the formation and development of "stabilising" kernels was observed which seems to be influenced primarily by additional aero-thermodynamic influences of preceding ignition kernels.
In summary, this study clearly resolves the general trends underlying the formation processes of the "first" kernels and improves the level of understanding of those processes.

ACKNOWLEDGMENTS

This work has been funded by ALSTOM Power Ltd. and the German Federal Ministry for Economic Affairs and Energy within the AG Turbo 2020 Research Program which is gratefully acknowledged. The authors would also like to thank S. Peukert, T. Schiek, R. Schieferstein and M. Kapernaum for their technical support and M. Stöhr for his support during the PIV measurements.

References

[1] Blouch J. D., Law C. K., Effects of turbulence on nonpremixed ignition of hydrogen in heated counterflow, Comb.Flame 132 (2003), pp. 512-522

[2] Mastorakos E., Ignition of turbulent non-premixed flames, Prog. Energy Comb. Science 35 (2009), pp. 57-97

[3] Markides C. N., Mastorakos E., Experimental Investigation of the Effects of Turbulence and Mixing on Autoignition Chemistry, Flow Turbulence Combust. (2011), 86:585-608

[4] Johannessen B., North A., Dibble R., Lovas T., Experimental studies of autoignition events in unsteady hydrogen-air flames, Comb. and Flame 162 (2016), pp. 3210-3219

[5] Markides C. N., Advanced Autoignition Theory, http://www2.eng.cam.ac.uk/ cnm24/images/Autoignition.pdf (accessed November 21st, 2016)

[6] Markides C. N., Mastorakos E., An experimental study of hydrogen autoignition in a turbulent co-flow of heated air, Proc. Comb. Institute 30 (2005), pp. 883-891

[7] Joos F., Brunner P., Schulte-Werning B., Syed K., Eroglu A., Development of the Sequential Combustion System for the ABB GT24/ GT26 Gas Turbine Family, ASME (1996) paper No. 1996-GT-315

[8] Güthe F., Hellat J., Flohr P., The Reheat Concept: The Proven pathway to Ultralow Emissions and High Efficiency and Flexibility, J. Eng. Turbines Power, 131 (2009), pp. 021503 1-7

[9] Wind T., Güthe F., Syed K., Co-firing of Hydrogen and Natural Gases In Lean Premixed Conventional and Reheat Burners (Alstom GT 26), ASME (2014) paper No. GT2014-25813

[10] Fleck J., Griebel P., Steinberg A. M., Stöhr M., Aigner M., Ciani A., Autoignition Limits of Hydrogen at Relevant Reheat Combustor Operating Conditions, J. Eng. Gas Turbines Power 134 (2012), pp. 041502 1-8

[11] Fleck J., Griebel P., Steinberg A. M., Arndt C. M., Naumann C., Aigner M., Autoignition of hydrogen/ nitrogen jets in vitiated air crossflows at different pressures, Proc. Combust. Inst. 34 (2013), pp. 3185-3192

[12] Schmalhofer C., Prause J., Griebel P., Fleck J., Stöhr M., Severin M., Aigner M., Wind T., Experimental and Numerical Investigation on Auto-Ignition of Hydrogen-Rich Fuels at Reheat Operating Conditions, Proceedings of The Future of Gas Turbine Technology, 7th International Conference, 2014

[13] Schmalhofer C., Griebel P., Stöhr M., Aigner M., Auto-ignition of in-line injected Hydrogen/ Nitrogen fuel mixtures at reheat combustor operating conditions, ASME (2015) paper No. GT2015-43414

[14] Dimotakis P. E., Two-Dimensional Shear-Layer Entrainment, AIAA Journal, Vol. 24 (1986), No. 11, pp. 1791-1796

[15] Dimotakis P. E., Turbulent free shear layer mixing and combustion, GALCIT Report FM91-2, 29 July 1991

[16] Dimotakis P. E., Turbulent Mixing, Annu. Rev. Fluid Mech. 2005, 37:329-56

[17] Fleck J. M., Griebel P., Steinberg A. M., Stöhr M., Aigner M., Ciani A., Experimental Investigation of a Generic, Fuel Flexible Reheat Combustor at Gas Turbine Operating Conditions, ASME (2010) Paper No. GT2010-22722

[18] Lückerath R., Meier W., Aigner M., FLOX® Combustion at High Pressure with Different Fuel Compositions, J. Eng. Gas Turbines Power, 130 (2008), pp. 011505 1-7

[19] Poyyapakkam M., Wood J., Mayers S., Ciani A., Güthe F., Syed, K., Hydrogen Combustion within a Gas Turbine Reheat Combustor, Proceedings of ASME Turbo Expo 2012, GT2012-69165

[20] ENCAP FP6 Project, http://www.encapco2.org/

[21] Stopper U., Aigner M., Meier W., Sadanandan R., Stöhr M. and Kim S. K., Flow Field and Combustion characterization of Premixed Gas Turbine Flames by Planar Laser Techniques, J. Eng. Gas Turbines Power, 131 (2009), pp. 021504 1-8

[22] Brown G. L., Roshko A., On density effects and large structure in turbulent mixing layers, J. Fluid Mech. (1974), vol. 64, part 4, pp. 775-816

[23] Hermanson J. C., Mungal M. G., Dimotakis P. E., Heat Release Effects on Shear-Layer Growth and Entrainment, AIAA Journal, Vol. 25 (1986), No. 4, pp. 578-583

[24] Mungal M. G., Dimotakis P. E., Broadwell J. E., Turbulent Mixing and Combustion in a Reacting Shear Layer, AIAA Journal, Vol. 22 (1984), No. 6, pp. 797-800